

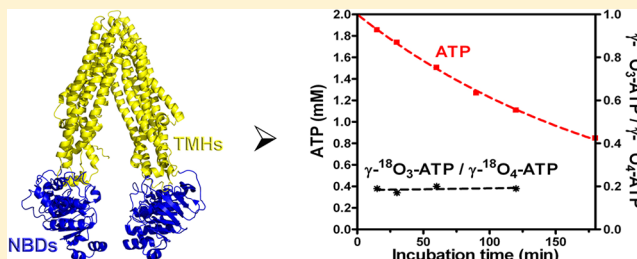
Reaction Dynamics of ATP Hydrolysis Catalyzed by P-Glycoprotein

Michele Scian,[#] Mauro Acchione,[#] Mavis Li, and William M. Atkins*

Department of Medicinal Chemistry, University of Washington, Box 357610, Seattle, Washington 98195-7610, United States

Supporting Information

ABSTRACT: P-glycoprotein (P-gp) is a member of the ABC transporter family that confers drug resistance to many tumors by catalyzing their efflux, and it is a major component of drug–drug interactions. P-gp couples drug efflux with ATP hydrolysis by coordinating conformational changes in the drug binding sites with the hydrolysis of ATP and release of ADP. To understand the relative rates of the chemical step for hydrolysis and the conformational changes that follow it, we exploited isotope exchange methods to determine the extent to which the ATP hydrolysis step is reversible. With $\gamma^{18}\text{O}_4$ -labeled ATP, no positional isotope exchange is detectable at the bridging β -phosphorus–O– γ -phosphorus bond. Furthermore, the phosphate derived from hydrolysis includes a constant ratio of three ^{18}O /two ^{18}O /one ^{18}O that reflects the isotopic composition of the starting ATP in multiple experiments. Thus, H_2O -exchange with HPO_4^{2-} (P_i) was negligible, suggesting that a $[\text{P-gp}\cdot\text{ADP}\cdot\text{P}_i]$ is not long-lived. This further demonstrates that the hydrolysis is essentially irreversible in the active site. These mechanistic details of ATP hydrolysis are consistent with a very fast conformational change immediately following, or concomitant with, hydrolysis of the γ -phosphate linkage that ensures a high commitment to catalysis in both drug-free and drug-bound states.



The ATP-binding cassette (ABC) transporters comprise a large family of transmembrane ATP-dependent efflux pumps that are best described by their shared “ATP-switch” mode of action.¹ In humans, the isoform ABCB1, or P-glycoprotein, plays a significant role in cellular drug resistance in tumors in which it is overexpressed, and it contributes to drug–drug interactions due to its high level expression in hepatic, renal, and intestinal tissue.^{2–6} As a result, there is significant interest in designing inhibitors of P-gp that could be used to modulate drug efflux, particularly in the central nervous system,⁷ and efforts to develop inhibitors could be facilitated by further understanding of the role of substrate–nucleotide binding and concomitant structural changes in transmembrane domains (TMDs) and nucleotide binding domains (NBDs) during the ATP catalytic cycle.

On the basis of structural models of murine and *Caenorhabditis elegans* proteins,^{8,9} the human P-gp likely consists of a dimer of two TMDs with six transmembrane helices (TMHs) that form a hydrophobic and promiscuous drug binding site, or sites with access to the plasma membrane inner leaflet (Figure 1). These sites are coupled functionally to two NBDs on the cytosolic side of the membrane that catalyze the hydrolysis of ATP. On the basis of the structural models, it has been suggested that the NBDs are brought into close proximity upon binding nucleotide,^{10,11} but the magnitude of functionally important conformational changes remains unknown. All three steps in the NBD cycle (ATP binding, hydrolysis, and release of products) are associated with release of energy coupled to some form of conformational change in either the TMDs or NBDs. Although mechanistic models differ in their details depending on the particular ABC transporter,

the available data indicate that ATP hydrolysis alternates between the two NBDs, and the hydrolysis, or dissociation of ADP, is used to drive distant conformational changes in the transmembrane helices, to allow drugs to be released to the extracellular surface and to “reset” the conformational state of the protein.^{12–15}

P-gp binds a remarkably wide range of drugs or probe ligands that differentially stimulate or inhibit the ATPase activity at saturating concentrations.¹⁶ In fact, several distinct binding sites have been proposed within the transmembrane helices, which may communicate allosterically despite their distinct selectivities.² These binding sites include residues on helices 4 and 5 and 10 and 11, and, taken together, they exhibit impressive promiscuity.¹⁷ On the basis of many biochemical data, it is likely that the large binding site within the TMDs includes subsites with overlapping but distinct substrate preferences, and this could result in multiple drug translocation pathways.^{18,19}

Despite major progress in our understanding of the human P-gp mechanism, including the availability of X-ray structures of closely related homologues,^{8,9} the molecular details of several aspects of the P-gp reaction cycle remain uncertain. For example, P-gp exhibits a basal ATP hydrolysis even in the absence of substrates or drug, but no physiological purpose is known for this activity. In addition, different substrates bind in different regions of the large promiscuous binding site, so it is challenging to understand how drugs bound at different sites can communicate with the NBDs to stimulate ATP hydrolysis.

Received: September 13, 2013

Revised: January 2, 2014

Published: February 7, 2014

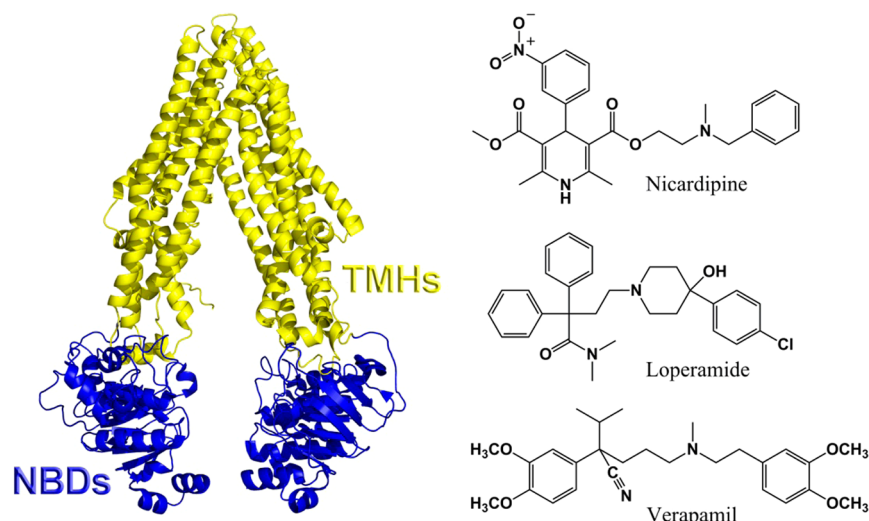


Figure 1. Left: Ribbon structure of murine P-gp (pdb: 3GSU) in the inward-facing nucleotide free state. The NBDs (blue) move into close proximity and the TMHs (yellow) rearrange upon nucleotide binding. Right: Chemical structures of three P-gp substrates studied in this work.

Although significant evidence indicates that the D-loops of the NBDs and helices 6 and 12 of the TMDs are important in the interdomain communication, it remains unknown how different substrates utilize a common mechanism or whether there are drug-dependent differences in the coupling between these domains.^{20–22}

P-gp poses an interesting example of ATP hydrolysis because it is widely proposed that release of ADP is rate limiting in the catalytic cycle,^{21,23,24} which implies a significant population of the [P-gp·ADP·P_i] or [P-gp·ADP] complex at steady state, where P_i is used throughout this manuscript to abbreviate HPO₄²⁻. In addition, there is a vast body of evidence that indicates that the enzyme undergoes significant conformational change immediately after ATP hydrolysis and prior to ADP release.^{15,22,26} The majority of data that support the posthydrolysis conformational change exploit a nonphysiologic “trapped state” with VO₄³⁻ ion replacing the P_i to form a pseudoirreversible complex. On the basis of the resulting mechanistic models, it is reasonable to expect that, if the release of ADP is sufficiently slow or incompletely coupled to formation of the posthydrolysis conformation, then the highly populated [P-gp·ADP·P_i] complex could regenerate ATP at a measurable rate, as observed for other classes of ATPases.^{27,28} On the other hand, if a sufficiently fast conformational change preceded ADP release, then no regeneration of ATP would be possible, and the hydrolysis step would be completely coupled to the subsequent conformational change. In effect, the relative rates of hydrolysis and conformational change are not well understood, yet they determine the commitment to catalysis once ATP is hydrolyzed.

Because many ATPases demonstrate substantial reversibility of the hydrolytic step, without full commitment to catalysis, particularly in the absence of one or more of their cosubstrates, we considered the possibility that P-gp could include a reversible component in the ATP hydrolysis. For other ATPases, such reversibility has been documented by NMR-based approaches as well as mass spectrometry which both rely on the rearrangement or “isomerization” of ¹⁸O in labeled ATP and is referred to as positional isotope exchange (PIX).^{27–32} Therefore, we performed NMR-based PIX experiments aimed to quantify the relative rate of regeneration of ATP from hydrolytic products ADP and P_i at the active sites of the NBDs.

With PIX experiments using γ -¹⁸O₄-ATP, it is possible to monitor the relocation of ¹⁸O label in the bridging position of the γ -phosphate of ATP into the nonbridging position on the β -phosphate, as a measure of reformation of the ATP from ADP and ¹⁶O-/¹⁸O-containing free phosphate ion (Figure 2). The extent of PIX that occurs is essentially a measure of the forward flux to the new conformation associated with the [P-gp·ADP·P_i] complex versus backward flux to the [P-gp·ATP] complex. PIX would not be observed if the new conformation that is populated immediately after hydrolysis differed significantly in the ATP binding sites. In addition, if the ATP hydrolysis of P-gp was reversible, then different [P-gp·ADP·P_i·drug] complexes would potentially yield varying amounts of PIX. In effect, a change in reversibility, if present, would provide a direct measure of the impact of different substrates or inhibitors on linking conformational changes with ATP hydrolysis.

A second measure of reaction dynamics for ATP hydrolysis has been exploited for many well-studied enzymes, wherein there is incorporation of additional water-borne oxygen atoms into the enzyme-bound P_i prior to release. If the [enzyme·ADP·P_i] complex is sufficiently long-lived, then additional rounds of H₂O attack at the P_i lead to further incorporation of oxygen from H₂O. We analyzed both PIX and H₂O exchange with P_i with human P-gp in liposomes. We report that no detectable PIX is observed in either the basal ATPase activity of P-gp or in the presence of the probe substrates nicardipine, verapamil, or loperamide, or the inhibitor cyclosporin A. Furthermore, none of the P_i in the [P-gp·ADP·P_i·drug] complex exchanges oxygen with water in any of the complexes studied. Thus, these data further support the model wherein there is fast conformational change immediately post hydrolysis, which allows for fast P_i release and a high commitment to catalysis in the NBDs.

■ MATERIALS AND METHODS

Materials. *n*-Dodecyl- β -D-maltopyranoside (DDM) was purchased from Affymetrix. His60 nickel affinity resin was from Clontech. *Escherichia coli* total lipid extract was purchased from Avanti Polar Lipids. C219 mouse IgG1 monoclonal antibody for immunoblots was from Covance. Goat antimouse IgG (H + L) secondary antibody, DyLight 800 conjugate was

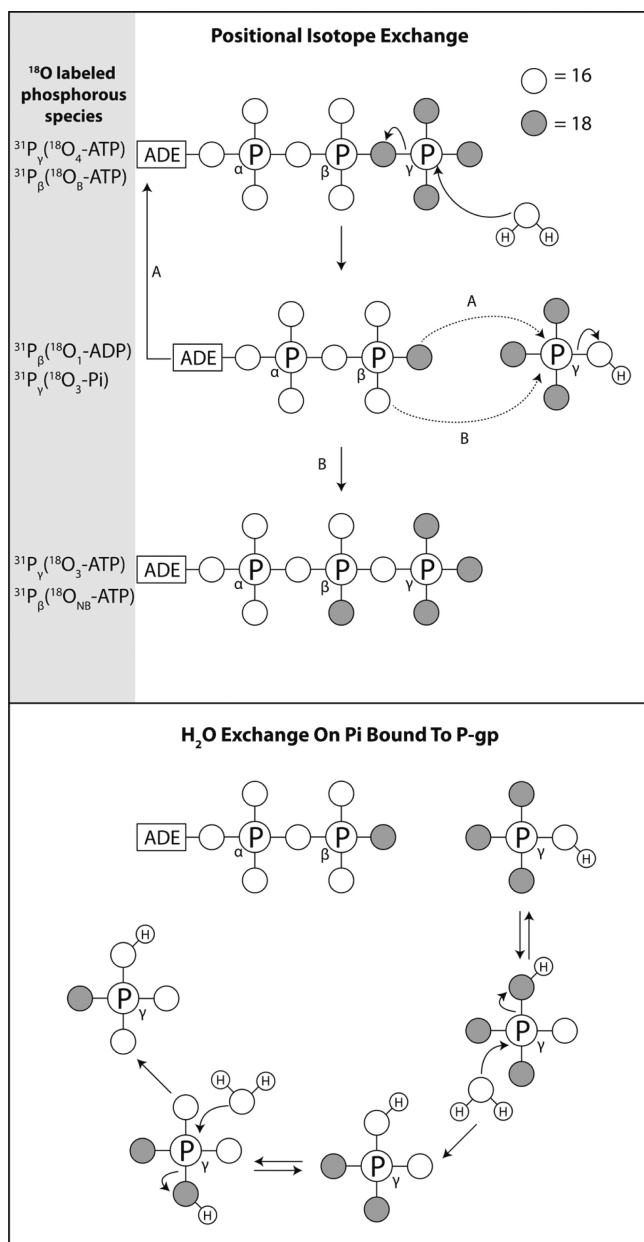


Figure 2. Top: Schematic of PIX. Open and shaded circles represent ¹⁶O and ¹⁸O, respectively. Starting with γ -¹⁸O₄-ATP with ¹⁸O at each of the γ -phosphorus positions, hydrolysis followed by isomerization and reformation of ATP (pathway B) yields ¹⁸O in the nonbridging (NB) versus the initial bridging (B) position of the β -phosphorus. Bottom: Schematic of H₂O exchange with P_i in the [P-gp·ADP·P_i] complex. Attack of H₂O on the P_i bound to P-gp leads to exchange of the ¹⁸O from the P_i with ¹⁶O.

from Thermo Scientific. Commercial P-gp supersomes were purchased from BD Biosciences.

Adenosine 5'-triphosphate sodium salt, γ -¹⁸O₄-ATP, with a per-site basis isotopic enrichment of at least 94% was purchased from Cambridge Isotopes.

Insect cell lines and expression medium were from Invitrogen. Cholesterol, chloroform, and all other reagents were from Sigma-Aldrich.

Baculovirus Expression of Human P-Glycoprotein (P-gp). The strains, expression constructs, and growth conditions

for expression of human P-gp in insect cells have been described previously.³³

Preparation of Supersomes or Microsomes. Throughout the manuscript the term “supersome” refers to microsomes obtained from insect cells that overexpress P-gp, and “microsome” refers to those obtained from “control” insect cells not overexpressing P-gp. *Trichoplusia ni* (*T.ni*) cells expressing P-gp were harvested by centrifugation and then resuspended in ice-cold hypotonic homogenization buffer (5 mM Tris, 5 mM TCEP, 40 μ M leupeptin, 2 μ M pepstatin A, 4 mM benzamidine, 200 μ M PMSF, pH 7.4) at a ratio of 5 mL of buffer per gram wet-weight of cells and incubated for 45 min on ice. All further steps were carried out at 4 °C or on ice. The mixture was lysed with a minimum of 10 strokes using a Potter-S homogenizer and then preclarified by spinning at 500g for 10 min. The supernatant was centrifuged at 20000g for 60 min. The supersome or microsome pellet was resuspended in a minimum of storage buffer (50 mM Tris, 250 mM sucrose, 20% w/v glycerol, 5 mM TCEP, 40 μ M leupeptin, 2 μ M pepstatin A, 4 mM benzamidine, 200 μ M PMSF, pH 7.4) and stored at -80 °C until further use. Aliquots were removed prior to freezing to determine total membrane protein concentration and test for drug-stimulated ATPase activity.

Colorimetric Determination of Drug-Stimulated ATPase Activity. Basal versus drug-stimulated ATPase reactions were carried out with various concentrations of ATP at 37 °C and quenched with 10 mM EDTA. Liberated phosphate was quantified by colorimetric assay³⁴ using phosphate standards and commercial P-gp-supersomes (BD Biosciences) as a positive control.

Solubilization and Purification of P-gp. Frozen supersomes were thawed quickly and then resuspended in solubilization buffer (2% w/v DDM, 50 mM Tris, 300 mM NaCl, 1.5 mM MgSO₄, 20 mM imidazole, 0.4% w/v *E. coli* lipids, 20% w/v glycerol, 5 mM TCEP, 40 μ M leupeptin, 2 μ M pepstatin A, 4 mM benzamidine, 200 μ M PMSF, pH 7.4). The mixture was homogenized by passing through a narrow 25-gauge syringe and then incubated at 4 °C with mixing for 1 h. The mixture was clarified by centrifugation at 10000g for 30 min at 15 °C and the supernatant transferred to pre-equilibrated His60 resin. The protein was batch adsorbed to the resin over 4 h at 4 °C and then washed extensively with equilibration buffer (0.1% w/v DDM, 50 mM Tris, 300 mM NaCl, 1.5 mM MgSO₄, 20 mM imidazole, 0.4% w/v *E. coli* lipids, 20% w/v glycerol, 5 mM TCEP, 40 μ M leupeptin, 2 μ M pepstatin A, 4 mM benzamidine, 200 μ M PMSF, pH 7.4). Next, the resin was washed with buffer containing 200 mM imidazole without protease inhibitors. Fractions containing pure P-gp were collected by eluting three times with 2 bed volumes each of 500 mM imidazole and lowering the pH from 7.4 to 6.8.

Preparation of P-gp Liposomes. Purified P-gp was incorporated into preformed liposomes as follows. *E. coli* lipids/cholesterol 4:1 films were resuspended in 50 mM Tris, 150 mM NaCl, pH 7.4 using a bath sonicator. The opaque mixture was subjected to several freeze-thaw cycles in liquid nitrogen prior to passing through a mini-extruder (Avanti Polar lipids) fitted with a 200 nm polycarbonate (PC) membrane. Detergent-saturated liposomes were used for P-gp-reconstitution, and the R_{sat} value was determined by titrating a sample of preformed liposomes with detergent and measuring the change in absorbance at 540 nm. When preparing detergent-saturated liposomes for mixing with purified P-gp, the R_{sat} value was adjusted to compensate for detergent and lipid present in

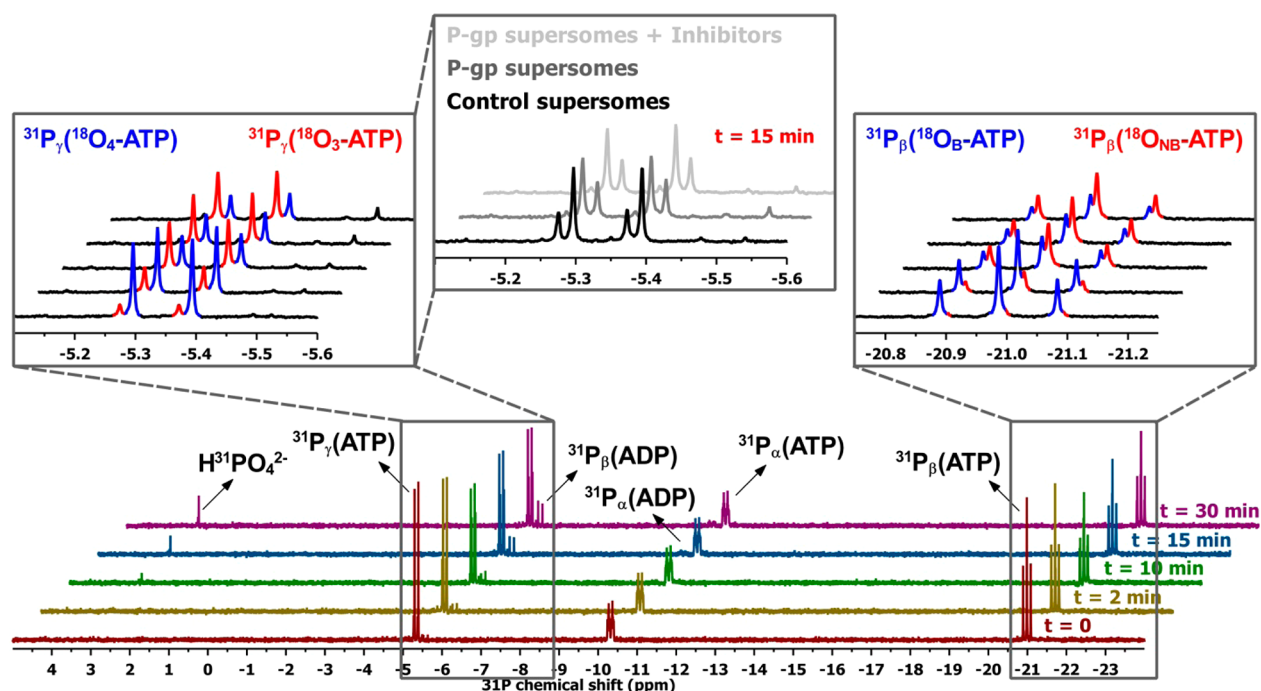


Figure 3. Positional isotope exchange with commercial human P-gp supersomes. Total proteins (28.2 $\mu\text{g}/\text{mL}$) were incubated with 2 mM $\gamma\text{-}^{18}\text{O}_4\text{-ATP}$, 50 mM Tris-HCl, 15 mM NH_4Cl , 5 mM MgSO_4 , 2.5 mM EGTA, 0.02 wt % NaN_3 , 2 mM TCEP, pH 7.4 in the presence of 50 μM nocardipine. For the samples with inhibitors (gray spectra top middle panel), conditions were as described in Materials and Methods. ^{31}P NMR spectra were recorded at the times indicated. In the left-hand inset, the $^{31}\text{P}_\gamma$ signals of ATP bearing four or three ^{18}O are presented in blue and red, respectively. The $^{31}\text{P}_\beta$ signals from ADP clearly demonstrate that ADP is formed concomitant with the changes in isotopic composition of the $^{31}\text{P}_\gamma$ signal (red vs blue). In the right-hand inset, the $^{31}\text{P}_\beta$ signals originating from ATP with ^{18}O at the bridging position ($^{18}\text{O}_\text{B}$) or at the nonbridging position ($^{18}\text{O}_\text{NB}$) are shown in blue and red, respectively.

purified P-gp sample. Upon mixing, the P-gp/detergent/liposome sample was incubated for 1 h with mixing. Detergent was removed by incubating the mixture with prewashed Amberlite-XAD beads that were prewashed with methanol and resuspended in buffer for a minimum of 2 h at 25 $^\circ\text{C}$, and the mixture was passed several times through a 200 nm PC membrane using an extruder. The resulting P-gp-liposome prep was stable at -80°C with no significant loss in ATPase activity.

Determination of Total Phosphorus in Phospholipids and Protein Concentration. Phospholipids were quantified based on the colorimetric assay recommended by Avanti Polar Lipids, Inc., using phosphate standards. Protein concentration was determined using trichloroacetic acid (TCA)/acetone protein precipitation, followed by Bio-Rad DC protein assay.

NMR Spectroscopy. All NMR experiments were performed at 25 $^\circ\text{C}$ on a 499.73 MHz Agilent DD2 spectrometer equipped with a 5-mm AutoX Dual Broadband, z-axis pulsed-field gradient probe head.

Solutions of 31 nM liposomes-reconstituted P-gp (200 nm *E. coli* lipids/cholesterol liposomes) were incubated at 37 $^\circ\text{C}$ with 2 mM $\gamma\text{-}^{18}\text{O}_4\text{-ATP}$, 50 mM Tris-HCl, 15 mM NH_4Cl , 5 mM MgSO_4 , 2.5 mM EGTA, 0.02 wt % NaN_3 , 2 mM TCEP, pH 7.4 in the absence (basal activity) or in presence (stimulated activity) of 50 μM nocardipine, loperamide or verapamil (from 10 mM stock solutions in dimethyl sulfoxide, Sigma-Aldrich). Inhibition of P-gp was studied with final concentrations of cyclosporin A of 20 μM , by dilution from a stock solution in DMSO, to yield a final DMSO concentration of 1%. Aliquots were taken at variable times, quenched by addition of 20 mM EDTA, pH adjusted to approximately 8.5 with 5 M NaOH, and spun at 14 000 rpm for 5 min to remove insoluble material. The

supernatant was transferred to a clean tube and D_2O added to a final concentration of 10% v/v. The final cosolvent content was <1% v/v. Adding EDTA quenched ATPase activity and sequestered all divalent cations to minimize the exchange broadening. A high pH value was also employed to minimize broadening due to protons exchange.³⁵

PIX positive control samples were prepared as above but using commercial human P-gp-supersomes (28.2 $\mu\text{g}/\text{mL}$ total protein, BD Gentest) or s9 insect cell-microsomes (28.2 $\mu\text{g}/\text{mL}$ total protein, BD Supersomes) and adding 2.5 mM EGTA to inhibit Ca^{2+} -dependent ATPases. Alternatively, to inhibit other major ATPases other than P-gp including Na^+/K^+ ATPases and F1, H^+/K^+ ATPases, 1 mM ouabain (Sigma-Aldrich), 8 mM sodium azide (Sigma-Aldrich), and 50 μM mellitin were used.

^{31}P NMR spectra (at 202.29 MHz) were acquired at a resolution of 16k complex points in the time domain with 2048 accumulations each (sw = 7062.1 Hz, d1 = 1.5 s). Data were zero filled to 32k points, and no apodization function was applied before Fourier transformation. Spectra were referenced to Phosphoric acid 85 wt % in H_2O (Sigma-Aldrich).

All data were processed and analyzed using MNovo 8.1 processing software (Mestrelab Research, Santiago de Compostela, Spain). All NMR experiments were performed at least four times on at least two different preparations of P-gp supersomes or P-gp liposomes.

RESULTS

To establish a PIX assay, “positive control” supersomes known to contain multiple ATPases were incubated for varying times with labeled ATP, where each oxygen atom attached to the γ

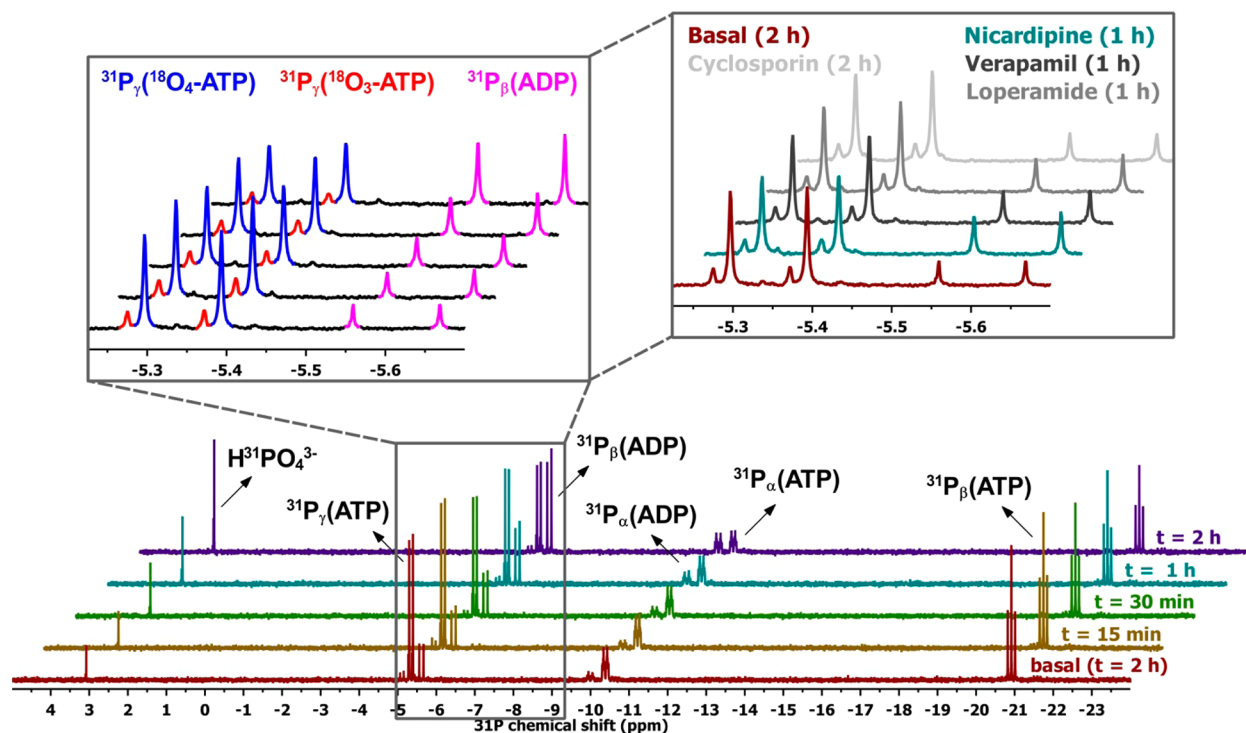


Figure 4. Absence of positional isotope exchange with purified liposome-reconstituted P-gp. 31 nM P-gp was incubated with 2 mM γ - $^{18}\text{O}_4$ -ATP, 50 mM Tris-HCl, 15 mM NH_4Cl , 5 mM MgSO_4 , 2.5 mM EGTA, 0.02 wt % NaN_3 , 2 mM TCEP, pH 7.4 in the presence of 50 μM nicardipine. The specific activity for the Nicardipine-stimulated P-gp was 1660 nmol of P_i /min/mg protein, at 2 mM ATP concentration, 37 $^\circ\text{C}$. The reactions were conducted as described in the text, and ^{31}P NMR spectra were recorded at the times indicated. The incubation was also conducted in the presence of 50 μM loperamide or 50 μM verapamil, or 20 μM cyclosporin A (right-hand side inset).

phosphorus was ^{18}O . The aim of these experiments was to demonstrate the feasibility of observing PIX with membrane ATPases in our hands, rather than to quantify PIX for any specific ATPase, and to determine if PIX due to P-gp could be detected in this environment. The ^{31}P nuclei of ATP were monitored by NMR; it is well established that the chemical shift of ^{31}P is sensitive to the oxygen isotope that is attached to it, and whether the oxygen isotope is in a position that bridges the γ and β phosphorus atoms or in a nonbridging position.²⁹ Specifically, the substitution of an ^{18}O for an ^{16}O induces a ~ 0.02 ppm (about 4 Hz at 202.93 MHz) downfield shift in the ^{31}P NMR resonance per oxygen substituted, while the effect of ^{18}O exchange from the $\beta\gamma$ -bridge position to a β -nonbridge position on the $^{31}\text{P}_\beta$ resonance is a less pronounced upfield shift (~ 0.01 ppm or about 2 Hz at 202.93 MHz). This enables PIX at the γ -phosphoryl group to be easily detected by inspection of the ^{31}P NMR spectrum. In fact, the ^{18}O exchange from the $\beta\gamma$ -bridge position to a β -nonbridge position results in a decrease in the signal of $^{31}\text{P}_\gamma$ with four bound ^{18}O and an increase in the signal for the $^{31}\text{P}_\gamma$ with three ^{18}O atoms (Figure 3).

After incubation of supersomes with ^{18}O -labeled ATP, the Mg^{2+} in the assay buffer was chelated with EDTA to eliminate the line broadening that results from rapid dissociation and association of Mg^{2+} to the ATP. For a series of incubations, the NMR spectra of the ATP were then collected at varying times. For supersomes with expressed P-gp, clear NMR signals from ADP were observed and increased in intensity with increasing time of incubation (Figure 3). In addition, the appearance of ^{18}O in the nonbridging position of the β -phosphorus was readily apparent. PIX was easily detected in commercial supersomes that contain overexpressed P-gp. Interestingly, for

several preparations of microsomes and P-gp supersomes, those containing overexpressed P-gp consistently demonstrated a clear increase in PIX compared to control supersomes (Figure 3). This suggested that P-gp was contributing significantly to the observed PIX. In order to determine whether other highly abundant ATPases contributed to the PIX, experiments were performed in the presence of 2.5 mM EGTA, to inhibit Ca^{2+} -dependent ATPases, and 1 mM ouabain, 50 μM melleitin and 8 mM sodium azide, to inhibit Na^+/K^+ ATPases and $\text{F}_1\text{H}^+/\text{K}^+$ ATPases. These inhibitors had no detectable effect on the observed PIX, suggesting the possibility that P-gp contributes significantly in the P-gp supersomes. Similarly, however, the addition of nicardipine at concentrations that stimulate purified P-gp had no effect on the overall ATPase activity or PIX of P-gp supersomes, indicating that P-gp is not a dominant source of ATPase activity or PIX in these membranes. Results shown in Figure 3 are representative. The degree of PIX in P-gp supersomes as measured by the ratio γ - $^{18}\text{O}_3$ -ATP/ γ - $^{18}\text{O}_4$ -ATP varied less than 10% between preparations and between experiments with the same preparation.

Apparently, multiple ATPases are active in these membranes and contribute to PIX, such that inhibition or stimulation of one or a few ATPases does not yield a detectable change.

After 30 min, 31.8% of the residual (nonhydrolyzed) ATP was γ - $^{18}\text{O}_4$ -ATP, 63.1% was present as γ - $^{18}\text{O}_3$ -ATP, 5.2% as γ - $^{18}\text{O}_2$ -ATP, and γ - ^{18}O -ATP was not detectable. Therefore, $\sim 63\%$ of the total residual ATP was exchanged after 30 min. At t_0 , γ - $^{18}\text{O}_4$ -ATP was $\sim 85.4\%$, and γ - $^{18}\text{O}_3$ -ATP was $\sim 14.6\%$. PIX clearly occurs with these P-gp supersomes, and the potential contribution of P-gp is discussed further below. Most importantly, these experiments demonstrated that PIX is observable in our hands.

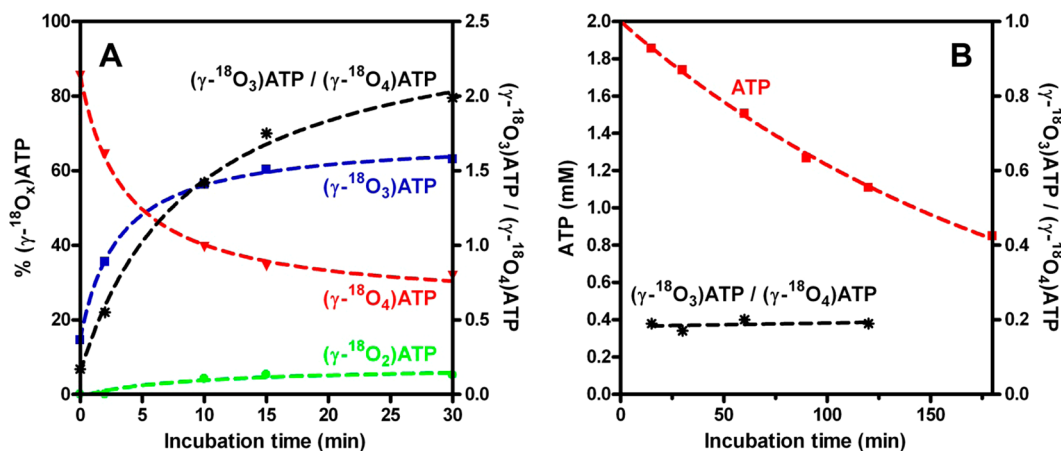


Figure 5. Rates of positional isotope exchange or ATP hydrolysis. (A) P-gp supersomes. The fractions of the exchanging species $\gamma\text{-}^{18}\text{O}_4$ -ATP in red, $\gamma\text{-}^{18}\text{O}_3$ -ATP in blue, and $\gamma\text{-}^{18}\text{O}_2$ -ATP in green as a function of the incubation time are shown. Also, the time dependence of the ratio $\gamma\text{-}^{18}\text{O}_3$ -ATP/ $\gamma\text{-}^{18}\text{O}_4$ -ATP is presented (black line). (B) Purified liposome-reconstituted P-gp. The hydrolysis rate (red line) and the time dependence of the ratio $\gamma\text{-}^{18}\text{O}_3$ -ATP/ $\gamma\text{-}^{18}\text{O}_4$ -ATP (black line) are shown. The reactions were conducted as described in the text, and ^{31}P NMR spectra were recorded at the times indicated. ATP concentrations and the PIX rates were determined from the areas of the ^{31}P NMR signals of the γ -phosphorus atom of ATP corresponding to the $\gamma\text{-}^{18}\text{O}_4$ -ATP, $\gamma\text{-}^{18}\text{O}_3$ -ATP, and $\gamma\text{-}^{18}\text{O}_2$ -ATP moieties.

Having established that we could observe PIX in a sample with our experimental protocol using the “positive control”, we examined purified P-gp reconstituted in liposomes. The purified protein was judged to be >90% pure based on gel electrophoresis (Supporting Information). In preparing P-gp reconstituted liposomes using purified P-gp expressed in insect cells, it was observed that using preformed liposomes to which detergent had been added to the saturation point (R_{sat}) increased the yield and activity of the preparation. The addition of TCEP as a reducing agent was also critical for maintaining stability in P-gp liposome preparations and activity in PIX experiments. These P-gp liposomes exhibited a 2.8–4.0-fold increase in ATPase activity with nocardipine compared to basal hydrolysis in the absence of drug, depending on the liposome preparation used.

In contrast to the P-gp supersomes, purified P-gp in liposomes exhibited no detectable PIX. Using ^{18}O -labeled ATP as above, the data for drug-free P-gp or in the presence of either 50 μM nocardipine, 50 μM loperamide or 50 μM verapamil or 20 μM cyclosporin A demonstrate no ^{18}O in the nonbridging position at any point during the time course of ATP hydrolysis (Figure 4). This is a remarkable result, inasmuch as many two-substrate enzymes that use ATP exhibit detectable reversibility in the hydrolysis.^{36,37} Notably, however, some ATPases yield no PIX.³¹

Exchange of Oxygen from H₂O into Phosphate Ion. As a second probe of the lifetime of the [P-gp·ADP·P_i] complex, we monitored the incorporation of ^{16}O from water into the P_i resulting from ATP hydrolysis. For some ATPases, further “attack” of water at P_i results in incorporation of multiple oxygen atoms from H₂O in addition to the one incorporated as a result of attack on the initial γ -phosphate of ATP. This occurs on the enzyme, but not in bulk solution, when active site features “activate” water as a nucleophile or P_i as an electrophile via specific or general acid or base catalysis.^{29,30} For each round of H₂O reaction with the P_i, an additional ^{16}O atom is incorporated (Figure 2). Thus, if no exchange occurs, the P_i will contain the single ^{16}O from the original ATP hydrolytic reaction. In the presence of P-gp liposomes, the fraction of P_i containing either two or three ^{16}O atoms reflected the isotopic

composition of the starting ATP, indicating no incorporation of ^{16}O resulting from a second or third attack of H₂O at this phosphorus, after the initial attack on ATP. Clearly, the P_i formed in the active site is highly protected from any “activated” H₂O, or it is rapidly released into bulk solution where the reaction is undetectably slow.

The combined results for the P-gp supersomes and P-gp liposomes are shown in Figure 5, which shows the time-dependent changes in the isotopically labeled species. Specifically, the concentration of ATP with three ^{18}O atoms on the γ -phosphorus ($\gamma\text{-}^{18}\text{O}_3$ -ATP), resulting from a single round of PIX, and the ATP with two ^{18}O atoms on the γ -phosphorus ($\gamma\text{-}^{18}\text{O}_2$ -ATP), resulting from two rounds of PIX, increase at the expense of starting $\gamma\text{-}^{18}\text{O}_4$ -ATP. The concentrations of species with two or three ^{18}O atoms in the ATP do change as ATP is depleted with P-gp in liposomes, as expected (Figure 4). The data for the concentration of ATP in the liposome experiment (Figure 5B) fit well to a first-order decay even at the longest time point of the experiments. This, combined with direct measurement of ATPase activity via the colorimetric assay in P-gp liposome samples incubated for times comparable to NMR experiments, indicates that no significant loss of enzyme activity occurred during the experiment. The first-order decrease in [ATP] (Figure 5B) reflects the non-steady-state nature of these experiments in which substrate depletion is significant by the end of experiments. It is useful to emphasize that, although the ATP concentration is changing in this experimental design, the ratio of $\gamma\text{-}^{18}\text{O}_3$ -ATP/ $\gamma\text{-}^{18}\text{O}_4$ -ATP is a valid indicator of PIX at low extent of ATP hydrolysis, unless there were a kinetic isotope effect favoring hydrolysis of the $\gamma\text{-}^{18}\text{O}_3$ -ATP. Such heavy atom isotope effects would be negligible in these experiments, and no significant kinetic selection for hydrolysis of initially reformed $\gamma\text{-}^{18}\text{O}_3$ -ATP is expected. Even if reversibly formed $\gamma\text{-}^{18}\text{O}_3$ -ATP were hydrolyzed preferentially, the ratio $\gamma\text{-}^{18}\text{O}_3$ -ATP/ $\gamma\text{-}^{18}\text{O}_4$ -ATP would be expected to increase, as it does with supersomes, where it changes from a value of ~0.2 to 2.0 in 30 min (Figure 5A black curve). The ratio does not change with P-gp liposomes (black curve in Figure 5B). As with the experiments with supersomes, the results with P-gp liposomes in Figures 4

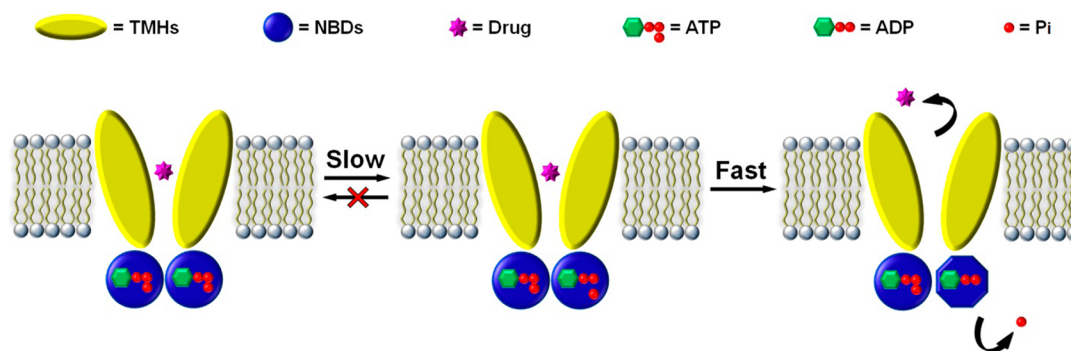


Figure 6. Schematized mechanism for conformational changes coupled to ATP hydrolysis in P-gp. A portion of the entire catalytic cycle is shown starting from the drug and nucleotide-bound state. After hydrolysis of one ATP, the conformational change and release of P_i are fast, preventing reformation of ATP or exchange of bound HPO_4^{2-} with H_2O . The conformational change is unlikely to include full dissociation of the NBD dimers but rather is fast with minor structural rearrangement. This conformational change is sufficient to ensure a high commitment to catalysis for ATP hydrolysis.

and 5 are representative; three preparations of P-gp liposomes demonstrated no PIX at comparable levels of ATPase activity.

DISCUSSION

Despite significant progress in understanding the mechanistic details of P-gp, few data report on the details of ATP hydrolysis and functionally important conformational changes in the protein that gate the release of spent nucleotide or drugs. The “vanadate-trapped” P-gp has provided a valuable model for the posthydrolysis [P-gp·ADP· P_i] state, and it is clear that this state is conformationally distinct from others throughout the reaction cycle.^{38–40} However, little is known about the reaction dynamics for the ATP hydrolysis step and the relative rates of chemical steps vs the conformational changes that follow. Although PIX studies are well established probes of ATP hydrolases, none have been reported for P-gp. The PIX and H_2O exchange experiments reported here are consistent with a few possible scenarios.

First, we discuss the results of the experiments with supersomes, for which some uncertainty exists regarding the contribution of P-gp to PIX. The observation that PIX occurs to a greater extent at equivalent degrees of ATP hydrolysis for the P-gp supersomes vs “normal” sf9 cell microsomes suggests that P-gp is either contributing to the PIX or its overexpression results in a change in levels of other ATPases that catalyze PIX. To determine whether other ATPases catalyze the PIX in these samples, incubations were performed with established inhibitors of Ca^{2+} -ATPases, Na^+/K^+ -ATPases, and the F1 H^+/K^+ ATPase. None of these inhibitors resulted in a decrease in PIX at any time point we examined, supporting the possibility that P-gp is responsible. However, it is extremely difficult to completely isolate PIX due to any specific enzyme in crude supersomes, so although these experiments are suggestive, they do not prove that P-gp in supersomes catalyzes PIX. Further experiments with mutants with altered ATPase activity may be useful to determine whether the P-gp contributes.

In contrast, the results with the P-gp liposomes are clear: no PIX occurs in this system. If the PIX in supersomes includes a contribution from P-gp, this difference obviously requires consideration. Possibly, the lipid environment of supersomes vs our liposomes could be sufficiently different to alter the catalytic properties of P-gp. Alternatively, other constituents of supersomes, including sterols or other proteins, could interact with P-gp and alter its properties. As above, further work is required to explore these possibilities. However, given the

definitive lack of PIX in P-gp liposomes, we discuss the implications of those results.

One possibility is that there is fast conformational change immediately after the initial hydrolysis step that prevents reversible formation of ATP, as summarized in Figure 6. In this case, conformational rearrangement to a state that is chemically incompetent for either reformation of ATP or for attack of water on the product P_i is significantly faster than either of these chemical processes. A second possibility is that P_i dissociates very rapidly, and this causes a subsequent conformational change that disfavors P_i rebinding and ATP synthesis. In either case, rapid changes in structure or ligand occupancy disfavor the reverse reaction.

Regarding the role of conformational change in P-gp catalysis, there are currently two competing models proposed to explain the events involved in drug efflux by P-gp that differ in the timing of drug/substrate release with ATP binding or hydrolysis. The first uses ATP binding and NBD dimerization as the pumping mechanism.^{41,42} Interaction of drug/substrate in the active site causes a conformational change in the NBDs that enhances ATP binding and initiates dimerization of the NBDs. This dimerization then results in another conformational change propagated to the TMDs, which open and expose the drug to the extracellular space. This TMD conformational change reduces affinity for the substrate allowing for its release. The next step in this model involves ATP hydrolysis to separate the NBD dimer and release P_i and ADP. In the other model, binding of ATP and substrate occur followed by hydrolysis of ATP at one NBD, which causes a conformational change that lowers affinity for the drug/substrate thereby releasing it.⁴³ Release of P_i and ADP is followed by hydrolysis of ATP at the second NBD resulting in a conformational change that resets the enzyme. In addition to the uncertainty concerning the timing of ATP hydrolysis relative to drug release, the magnitude of the conformational changes that take place during the catalytic cycle is debated. The crystal structures of the nucleotide-free murine P-gp or its homologue from *C. elegans* suggest that the inward-facing conformation to which drugs bind has the NBDs very far apart with no inter-NBD contact.^{8,9} However, cross-linking studies in which the NBDs are tethered suggest that their full dissociation from one another is not required for P-gp function.⁴⁴

Although the evidence for a significant posthydrolysis conformational change is abundant, it remains unknown whether the conformations observed in the crystal structures

are physiologically relevant. In fact, recent MD simulations based on crystal structures of NBD domains from the Sav1866 homologue suggest a detailed mechanism in which more localized conformational changes are sufficient to allosterically communicate with the drug binding sites and release ADP.¹⁷ In those studies, the ATP/ATP structure (ATP bound in each of the two sites at the NBD–NBD interface) was used as a starting point, and one ATP was removed to yield an ATP/apo NBD dimer. The highly conserved D-loop of the ATP-bound site was observed to undergo a conformational switch to allow hydrogen bonding between a conserved glutamate with a water molecule, which also hydrogen bonded to the backbone of the other D-loop of the other NBD. This oriented the water molecule for in-line displacement of ADP from the γ -phosphate of ATP. The rearrangement of the D-loop occurs with movement of other elements, which are thought to communicate with the TMHs, suggesting a mechanism for communication between the local reaction trajectory and the drug binding sites. However, for the ATP/ADP structure, with one ATP and one ADP bound, this conformational change to favor ATP hydrolysis did not take place. Thus, the MD simulations suggest that large scale conformational changes, to fully dissociated NBDs observed in the crystal structures, are not required to release ADP or drug. Such a full dissociation of the NBDs from the original nucleotide-bound NBD dimer conformation would be expected to be slow due to the need to disrupt many inter-NBD contacts. In turn, a slow dissociation would likely occur with a low commitment to catalysis by the NBDs with significant reversibility, in contrast to our observations here. In addition, other water molecules did not rearrange to provide additional nucleophilic waters in the vicinity. Thus, the PIX and H₂O exchange data support these MD simulations, requiring only local conformational changes to disrupt the ATP hydrolysis machinery, which happen fast relative to chemical steps. Notably, our experiments report only on the aggregate ATP hydrolysis at both sites. However, the data do indicate that *neither* ATP hydrolysis event is reversible *nor* yields a long-lived [P-gp·ADP·P_i] complex. If either ATP site yielded PIX or H₂O exchange, it would be observed. Figure 6 schematically demonstrates the relative rates of conformational change and chemical steps that are consistent with, but not proven by, the PIX results.

A second possible interpretation of the PIX and H₂O exchange results is that ADP and P_i are bound so rigidly that no rearrangement of oxygen ligands on phosphorus is possible. In principle, if all atoms were sufficiently immobilized with respect to their orientation on the phosphorus atoms, then the ¹⁸O oxygen atom of initially formed β -phosphate of ADP that was initially the bridging oxygen of γ -phosphate of ATP could attack the bound P_i and release the ¹⁶O atom derived from solvent, thus reforming γ -¹⁸O₄-ATP. This would yield no PIX despite reversible ATP hydrolysis. Similarly for the water exchange with P_i, it is possible that the P_i could be rigidly held so that even if the water exchanged with it, it could be displaced upon reversible reformation of the fully labeled ¹⁸O₄-ATP. A few observations suggest that these formal possibilities are unlikely. Rapid pseudo rotation of phosphorus ligands in hydrolysis reactions is common, wherein oxygen atoms readily exchange between positions in pentavalent phosphorus en route to hydrolysis products. Also, ADP and P_i have low binding affinities for P-gp and therefore would be expected to be able to “tumble” to some degree and allow for rearrangement of the oxygen atoms. For these reasons, we propose the

lack of PIX or H₂O exchange in the liposome experiments represents irreversibility, or very low reversibility, of ATP hydrolysis, rather than rigidly held hydrolysis products.

To the extent that this is the case, it is interesting that PIX and H₂O exchange with P_i are absent in both the drug-free P-gp and with several different drugs bound. A hallmark of P-gp is its extraordinary promiscuity wherein it couples ATP hydrolysis with transport of a remarkable range of structurally unrelated substrates. Presumably, different drugs lead to different conformations of the TMHs, and this prompted the expectation that different drugs could promote PIX or H₂O exchange to different extents. However, the results indicate that P-gp is able to ensure a high commitment to catalysis for each ATPase half reaction for the drug-free state as well as with the structurally distinct drugs we examined. This is particularly interesting in comparison to ATPases that demonstrate PIX or H₂O exchange with P_i at appreciable rates.²⁵ Typically, PIX is maximal when a cosubstrate is not present.²⁸ Such enzymes appear “perched” to optimize rates of ATP hydrolysis when cosubstrate is added but exhibit a high degree of reversible ATP hydrolysis, possibly, to minimize wasteful expenditure of ATP. That is, they are “perched” to optimize rates of ATP hydrolysis in the presence of cosubstrate and to minimize wasteful hydrolysis in their absence. To the extent that the vast array of drug substrates recognized by P-gp represent “cosubstrates”, measurable PIX would be expected in the absence of any drug. However, the basal ATPase activity exhibited no PIX or H₂O exchange. Unlike other ATPases, P-gp does not minimize or reduce wasteful ATP consumption with a reversible reaction manifold with drug-dependent increase in the commitment to catalysis. This further amplifies the enigmatic role, if any, of the basal ATPase activity of P-gp.

■ ASSOCIATED CONTENT

📄 Supporting Information

Results for gel electrophoresis with purified P-gp. This material is available free of charge via the Internet at <http://pubs.acs.org>.

■ AUTHOR INFORMATION

Corresponding Author

*E-mail: winky@uw.edu. Phone: 206-685-0379.

Author Contributions

#M.S. and M.A. contributed equally to this work.

Funding

This work was supported by NIH GM098457 (W.M.A.) and by the Department of Medicinal Chemistry.

Notes

The authors declare no competing financial interest.

■ ACKNOWLEDGMENTS

PIX experiments were performed at the University of Washington Analytical Biopharmacy Core, which is supported by the Washington State Life Sciences Discovery Fund and the Center for the Intracellular Delivery of Biologics.

■ ABBREVIATIONS

EGTA, ethylene glycol tetraacetic acid; EDTA, ethylene diaminetetraacetic acid; NBDs, nucleotide binding domains; TCEP, tris(2-carboxyethyl)phosphine; PC membrane, polycarbonate membrane; PIX, positional isotope exchange; PMSE, phenylmethanesulfonyl fluoride; TMDs, transmembrane domains

REFERENCES

- (1) Jones, P. M., O'Mara, M. L., and George, A. M. (2009) ABC transporters: a riddle wrapped in a mystery inside an enigma. *Trends Biochem. Sci.* 34, 520–531.
- (2) Lugo, M. R., and Sharom, F. J. (2005) Interaction of LDS-751 and rhodamine 123 with P-glycoprotein: evidence for simultaneous binding of both drugs. *Biochemistry* 44, 14020–14029.
- (3) Gillet, J. P., and Gottesman, M. M. (2010) Mechanisms of multidrug resistance in cancer. *Methods Mol. Biol.* 596, 47–76.
- (4) Gottesman, M. M. (2002) Mechanisms of cancer drug resistance. *Annu. Rev. Med.* 53, 615–627.
- (5) Juliano, R. (1976) Drug-resistant mutants of Chinese hamster ovary cells possess an altered cell surface carbohydrate component. *J. Supramol. Struct.* 4, 521–526.
- (6) Sharom, F. J. (2011) The P-glycoprotein multidrug transporter. *Essays Biochem.* 50, 161–178.
- (7) Jeynes, B., and Provias, J. (2011) An investigation into the role of P-glycoprotein in Alzheimer's disease lesion pathogenesis. *Neurosci. Lett.* 487, 389–393.
- (8) Aller, S. G., Yu, J., Ward, A., Weng, Y., Chittaboina, S., Zhuo, R., Harrell, P. M., Trinh, Y. T., Zhang, Q., Urbatsch, I. L., and Chang, G. (2009) Structure of P-glycoprotein reveals a molecular basis for poly-specific drug binding. *Science* 323, 1718–1722.
- (9) Jin, M. S., Oldham, M. L., Zhang, Q., and Chen, J. (2012) Crystal structure of the multidrug transporter P-glycoprotein from *Caenorhabditis elegans*. *Nature* 490, 566–569.
- (10) Sonveaux, N., Shapiro, A. B., Goormaghtigh, E., Ling, V., and Ruyschaert, J. M. (1996) Secondary and tertiary structure changes of reconstituted P-glycoprotein. A Fourier transform attenuated total reflection infrared spectroscopy analysis. *J. Biol. Chem.* 271, 24617–24624.
- (11) Qu, Q., Russell, P. L., and Sharom, F. J. (2003) Stoichiometry and affinity of nucleotide binding to P-glycoprotein during the catalytic cycle. *Biochemistry* 42, 1170–1177.
- (12) Callaghan, R., Ford, R. C., and Kerr, I. D. (2006) The translocation mechanism of P-glycoprotein. *FEBS Lett.* 580, 1056–1063.
- (13) George, A. M., and Jones, P. M. (2012) Perspectives on the structure-function of ABC transporters: the Switch and Constant Contact models. *Prog. Biophys. Mol. Biol.* 109, 95–107.
- (14) Sauna, Z. E., Smith, M. M., Muller, M., Kerr, K. M., and Ambudkar, S. V. (2001) The mechanism of action of multidrug-resistance-linked P-glycoprotein. *J. Bioenerg. Biomembr.* 33, 481–491.
- (15) Urbatsch, I. L., Tyndall, G. A., Tomblin, G., and Senior, A. E. (2003) P-glycoprotein catalytic mechanism: studies of the ADP-vanadate inhibited state. *J. Biol. Chem.* 278, 23171–23179.
- (16) Polli, J. W., Wring, S. A., Humphreys, J. E., Huang, L., Morgan, J. B., Webster, L. O., and Serabjit-Singh, C. S. (2001) Rational use of in vitro P-glycoprotein assays in drug discovery. *J. Pharmacol. Exp. Ther.* 299, 620–628.
- (17) Jones, P. M., and George, A. M. (2012) Role of the D-loops in allosteric control of ATP hydrolysis in an ABC transporter. *J. Phys. Chem. A* 116, 3004–3013.
- (18) Parveen, Z., Stockner, T., Bentele, C., Pferschy, S., Kraupp, M., Freissmuth, M., Ecker, G. F., and Chiba, P. (2011) Molecular dissection of dual pseudosymmetric solute translocation pathways in human P-glycoprotein. *Mol. Pharmacol.* 79, 443–452.
- (19) Rautio, J., Humphreys, J. E., Webster, L. O., Balakrishnan, A., Keogh, J. P., Kunta, J. R., Serabjit-Singh, C. J., and Polli, J. W. (2006) In vitro p-glycoprotein inhibition assays for assessment of clinical drug interaction potential of new drug candidates: a recommendation for probe substrates. *Drug Metab. Dispos.* 34, 786–792.
- (20) Crowley, E., O'Mara, M. L., Kerr, I. D., and Callaghan, R. (2010) Transmembrane helix 12 plays a pivotal role in coupling energy provision and drug binding in ABCB1. *FEBS J.* 277, 3974–3985.
- (21) Kerr, K. M., Sauna, Z. E., and Ambudkar, S. V. (2001) Correlation between steady-state ATP hydrolysis and vanadate-induced ADP trapping in Human P-glycoprotein. Evidence for ADP release as the rate-limiting step in the catalytic cycle and its modulation by substrates. *J. Biol. Chem.* 276, 8657–8664.
- (22) Storm, J., O'Mara, M. L., Crowley, E. H., Peall, J., Tieleman, D. P., Kerr, I. D., and Callaghan, R. (2007) Residue G346 in transmembrane segment six is involved in inter-domain communication in P-glycoprotein. *Biochemistry* 46, 9899–9910.
- (23) Syberg, F., Suveyzdis, Y., Kotting, C., Gerwert, K., and Hofmann, E. (2012) Time-resolved Fourier transform infrared spectroscopy of the nucleotide-binding domain from the ATP-binding Cassette transporter MsbA: ATP hydrolysis is the rate-limiting step in the catalytic cycle. *J. Biol. Chem.* 287, 23923–23931.
- (24) Verhalen, B., Ernst, S., Borsch, M., and Wilkens, S. (2012) Dynamic ligand-induced conformational rearrangements in P-glycoprotein as probed by fluorescence resonance energy transfer spectroscopy. *J. Biol. Chem.* 287, 11112–11127.
- (25) Bagshaw, C. R., Trentham, D. R., Wolcott, R. G., and Boyer, P. D. (1975) Oxygen exchange in the gamma-phosphoryl group of protein-bound ATP during Mg^{2+} -dependent adenosine triphosphatase activity of myosin. *Proc. Natl. Acad. Sci. U. S. A.* 72, 2592–2596.
- (26) Ramachandra, M., Ambudkar, S. V., Chen, D., Hrycyna, C. A., Dey, S., Gottesman, M. M., and Pastan, I. (1998) Human P-glycoprotein exhibits reduced affinity for substrates during a catalytic transition state. *Biochemistry* 37, 5010–5019.
- (27) Fan, F., Williams, H. J., Boyer, J. G., Graham, T. L., Zhao, H., Lehr, R., Qi, H., Schwartz, B., Raushel, F. M., and Meek, T. D. (2012) On the catalytic mechanism of human ATP citrate lyase. *Biochemistry* 51, 5198–5211.
- (28) von der Saal, W., Crysler, C. S., and Villafranca, J. J. (1985) Positional isotope exchange and kinetic experiments with *Escherichia coli* guanosine-5'-monophosphate synthetase. *Biochemistry* 24, 5343–5350.
- (29) Cohn, M., and Hu, A. (1978) Isotopic (^{18}O) shift in 31P nuclear magnetic resonance applied to a study of enzyme-catalyzed phosphate-phosphate exchange and phosphate (oxygen)-water exchange reactions. *Proc. Natl. Acad. Sci. U. S. A.* 75, 200–203.
- (30) Hackney, D. D., and Boyer, P. D. (1978) Evaluation of the partitioning of bound inorganic phosphate during medium and intermediate phosphate in equilibrium water oxygen exchange reactions of yeast inorganic pyrophosphatase. *Proc. Natl. Acad. Sci. U. S. A.* 75, 3133–3137.
- (31) Thomas, J., Fishovitz, J., and Lee, I. (2010) Utilization of positional isotope exchange experiments to evaluate reversibility of ATP hydrolysis catalyzed by *Escherichia coli* Lon protease. *Biochem. Cell Biol.* 88, 119–128.
- (32) Williams, L., Fan, F., Blanchard, J. S., and Raushel, F. M. (2008) Positional isotope exchange analysis of the Mycobacterium smegmatis cysteine ligase (MshC). *Biochemistry* 47, 4843–4850.
- (33) Ritchie, T. K., Grinkova, Y. V., Bayburt, T. H., Denisov, I. G., Zolnerciks, J. K., Atkins, W. M., and Sliagar, S. G. (2009) Chapter 11 - Reconstitution of membrane proteins in phospholipid bilayer nanodiscs. *Methods Enzymol.* 464, 211–231.
- (34) Chifflet, S., Torriglia, A., Chiesa, R., and Tolosa, S. (1988) A method for the determination of inorganic phosphate in the presence of labile organic phosphate and high concentrations of protein: application to lens ATPases. *Anal. Biochem.* 168, 1–4.
- (35) Raushel, F. M., and Villafranca, J. J. (1988) Positional isotope exchange. *Crit. Rev. Biochem.* 23, 1–26.
- (36) Midelfort, C. F., and Rose, I. A. (1976) A stereochemical method for detection of ATP terminal phosphate transfer in enzymatic reactions. Glutamine synthetase. *J. Biol. Chem.* 251, 5881–5887.
- (37) Raushel, F. M., and Villafranca, J. J. (1980) P-31 Nuclear Magnetic-Resonance Application to Positional Isotope Exchange-Reactions Catalyzed by *Escherichia coli* Carbamoyl-Phosphate Synthetase - Analysis of Forward and Reverse Enzymatic-Reactions. *Biochemistry* 19, 3170–3174.
- (38) Urbatsch, I. L., Sankaran, B., Weber, J., and Senior, A. E. (1995) P-glycoprotein is stably inhibited by vanadate-induced trapping of nucleotide at a single catalytic site. *J. Biol. Chem.* 270, 19383–19390.

(39) Rothnie, A., Storm, J., Campbell, J., Linton, K. J., Kerr, I. D., and Callaghan, R. (2004) The topography of transmembrane segment six is altered during the catalytic cycle of P-glycoprotein. *J. Biol. Chem.* 279, 34913–34921.

(40) Ritchie, T. K., Kwon, H., and Atkins, W. M. (2011) Conformational analysis of human ATP-binding cassette transporter ABCB1 in lipid nanodiscs and inhibition by the antibodies MRK16 and UIC2. *J. Biol. Chem.* 286, 39489–39496.

(41) Higgins, C. F., and Linton, K. J. (2004) The ATP switch model for ABC transporters. *Nat. Struct. Mol. Biol.* 11, 918–926.

(42) Linton, K. J., and Higgins, C. F. (2007) Structure and function of ABC transporters: the ATP switch provides flexible control. *Pflugers Arch.* 453, 555–567.

(43) Ambudkar, S. V., Kim, I. W., and Sauna, Z. E. (2006) The power of the pump: mechanisms of action of P-glycoprotein (ABCB1). *Eur. J. Pharm. Sc.* 27, 392–400.

(44) Verhalen, B., and Wilkens, S. (2011) P-glycoprotein retains drug-stimulated ATPase activity upon covalent linkage of the two nucleotide binding domains at their C-terminal ends. *J. Biol. Chem.* 286, 10476–10482.